

Quartz Sand Filter Media with Special Wettability for Continuous and Efficient Oil/Water Separation and Dye Adsorption

Authors:

Bigui Wei, Xuying Luo, Xiaosan Song, Hanyue Guo, Liang Dai, Hongwei Zhang, Gang Wang

Date Submitted: 2021-02-22

Keywords: quartz sand, continuous filtration, dye adsorption, oil/water separation, underoil highly hydrophobic, underwater superoleophobic

Abstract:

For continuous and efficient oil/water separation and adsorption of dyes, coconut shell powder was grafted onto the surface of quartz sand by dip-coating method to make coconut shell powder-covered quartz sand filter media (CSQS) with superhydrophilic and underwater superoleophobic properties and superoleophilic and underoil highly hydrophobic properties. The contact angles of the underwater oil and underoil water with CSQS were more than 151.2° and 134.2° , respectively. A continuous oil/water separation device was designed. The separation device filled with CSQS can separate oil/water mixture (whether heavy or light oil) into water and oil at the same time with a separation efficiency of above 99.92%. The filter layer can be recovered through reverse extrusion even after lyophobic liquid penetrated the filter layer; hence, the separation efficiency of the filter layer was still above 99.99% for diesel and water mixture. Simultaneously, CSQS can effectively adsorb methylene blue with the highest removal rate as 98.94%. CSQS can maintain stable wettability under harsh environment conditions. This paper provides a new idea on continuous and efficient oil/water separation and simultaneous dye adsorption.

Record Type: Published Article

Submitted To: LAPSE (Living Archive for Process Systems Engineering)

Citation (overall record, always the latest version):

LAPSE:2021.0074

Citation (this specific file, latest version):

LAPSE:2021.0074-1

Citation (this specific file, this version):


LAPSE:2021.0074-1v1

DOI of Published Version: <https://doi.org/10.3390/pr8091083>

License: Creative Commons Attribution 4.0 International (CC BY 4.0)

Article

Quartz Sand Filter Media with Special Wettability for Continuous and Efficient Oil/Water Separation and Dye Adsorption

Bigui Wei ^{1,2,*}, Xuying Luo ^{1,2}, Xiaosan Song ^{1,2}, Hanyue Guo ^{1,2}, Liang Dai ^{1,2},
Hongwei Zhang ^{1,2}  and Gang Wang ^{1,2}

¹ School of Environmental and Municipal Engineering, Lanzhou Jiaotong University, Lanzhou 730070, China; luoxy4523@163.com (X.L.); songxs@mail.lzjtu.cn (X.S.); guo13017652238@163.com (H.G.); dailiang818@mail.lzjtu.cn (L.D.); zhw@mail.lzjtu.cn (H.Z.); gangw99@mail.lzjtu.cn (G.W.)

² Key laboratory of Yellow River Water Environment in Gansu Province, Lanzhou 730070, China

* Correspondence: weibg@mail.lzjtu.cn; Tel.: +931-4956017

Received: 11 August 2020; Accepted: 31 August 2020; Published: 2 September 2020



Abstract: For continuous and efficient oil/water separation and adsorption of dyes, coconut shell powder was grafted onto the surface of quartz sand by dip-coating method to make coconut shell powder-covered quartz sand filter media (CSQS) with superhydrophilic and underwater superoleophobic properties and superoleophilic and underoil highly hydrophobic properties. The contact angles of the underwater oil and underoil water with CSQS were more than 151.2° and 134.2°, respectively. A continuous oil/water separation device was designed. The separation device filled with CSQS can separate oil/water mixture (whether heavy or light oil) into water and oil at the same time with a separation efficiency of above 99.92%. The filter layer can be recovered through reverse extrusion even after lyophobic liquid penetrated the filter layer; hence, the separation efficiency of the filter layer was still above 99.99% for diesel and water mixture. Simultaneously, CSQS can effectively adsorb methylene blue with the highest removal rate as 98.94%. CSQS can maintain stable wettability under harsh environment conditions. This paper provides a new idea on continuous and efficient oil/water separation and simultaneous dye adsorption.

Keywords: underwater superoleophobic; underoil highly hydrophobic; oil/water separation; dye adsorption; continuous filtration; quartz sand

1. Introduction

The composition of wastewater discharge has become complex and diverse with the rapid development of industry and agriculture. A large number of oil, water-soluble dyes, pesticides, and heavy metal pollutants will cause great harm to the environment if not effectively treated [1]. About 6 million tons of oil are discharged into the ocean every year because of crude oil leakage and pose a serious threat to microbial communities and marine organisms [2–6]. A large number of industrial oily wastewater is discharged into the water body and transferred to the food chain, which eventually affects public health. More than 7105 tons of synthetic dyes are produced annually and used in the textile, food, beverage, leather, pharmaceutical, and cosmetic industries, as well as printing ink, plastic, paint, and wood dye industries [7]. In addition, about 0.28 million tons of textile dyes are discharged into the water body through industrial wastewater every year and have led to the decrease in water transparency and oxygen solubility. As a result, ecological balance is destroyed. Dyes that enter water bodies, especially drinking water, will be ingested by humans and increase the risks of carcinogenesis, teratogenesis, and mutation [8]. Wastewater from the textile industry contains colored dyes and oil. Therefore, a material that can remove oil and dyes in wastewater from different industries

is urgently needed. Traditional treatment methods, such as membrane separation, chemical oxidation, advanced oxidation technology and biological process, have many applications in the industry but have some disadvantages, such as long treatment cycle, high energy consumption, and high treatment cost [9–11]. Special wettable materials have different wetting behaviors for oil and water and thus can be used for oil/water separation. Hydrophilic groups can also be used for dye adsorption [12–17].

Wettability is controlled by the chemical composition of the surface and micro/nanoscale surface structures [18–21]. Inspired by bionics, Jiang et al. [22] prepared super hydrophobic and super oleophilic stainless steel mesh film by forming hierarchical micro/nanostructured surfaces through covalent grafting and the self-assembly of hydrophobic groups to successfully and effectively separate oil/water mixture. Cheng et al. [23] prepared superhydrophobic and superhydrophilic film modified by graphene oxide and polydopamine to separate water/chloroform mixture. The superoleophilic materials that allow oil to penetrate and block water from passing through are called deoiling materials [16,24–28], which are suitable for the separation of heavy oil/water mixture. The superhydrophilic and superoleophobic underwater materials work in the opposite manner. In the premise of water pre-wetting, the water phase can penetrate the surface smoothly whereas the oil phase cannot adhere to the material called dewatering material [29–31]. Yu et al. [32] prepared a ceramic microfiltration membrane with superhydrophilic and underwater superoleophobic properties. The efficiency of separating oil-in-water emulsion was more than 99%. The superhydrophilic membrane is suitable for the separation of light oil/water mixture and solves the problem in water surfaces that are easily polluted by oil. The water phase or oil phase that cannot penetrate deoiling or dewatering materials will accumulate on the material continuously with the extension of separation time. The maximum invasion pressure of the material surface may be exceeded if the accumulation is not removed in time. In this case, discontinuous operation is adopted, that is, filtration is stopped first, the accumulated liquid is poured out, and then filtration is resumed. The practical application of superhydrophilic and superoleophilic materials is limited in the discontinuous operation process.

Some researchers have designed a three-way separation device for oil/water separation by combining a superhydrophilic and underwater superoleophobic material with a superhydrophobic and superoleophilic material [33–35]. Chen et al. [33] used two superwetting $\text{Co}_3\text{O}_4/\text{Ni}$ sponge to separate chloroform/water mixture. The test efficiency is above 97%. Li et al. [34] prepared two superwetting stainless steel meshes. The separator was used for the cyclic filtration of 120 mL of oil/water mixture by 50 times with an efficiency of over 99.8%. Xie et al. [35] used two superwetting stainless steel meshes to continuously separate 5 L of oil/water mixture. The efficiency is over 99.3%. Previous studies have shown that the separation effect is good. However, the volume of oil and water in continuous filtration is small, and these studies did not mention whether the filtration volume will be penetrated by lyophobic liquid if the filtration volume is too high and how the filter layer recovers after penetration. Therefore, this paper proposes a super-wetting quartz sand to continuously filter multiple liters of oil/water mixture, and a solution to restore the filter layer after penetration is proposed.

The superhydrophilic and underwater superoleophobic material and the superoleophilic and underoil highly hydrophobic material are superhydrophilic and superoleophilic in air. The preparation of superhydrophilic and superoleophilic surfaces can be achieved by introducing hydrophilic and lipophilic groups on the surface of materials and constructing rough structures at the same time. Forestry and agricultural residues are composed of cellulose, hemicellulose, and lignin, which contain more hydrophilic and lipophilic groups, such as $-\text{OH}$ and $-\text{COOH}$ [36]. Hence, these residues are ideal surface preparation materials with special wettability.

In this paper, coconut shell powder was coated on quartz sand to prepare quartz sand filter media with superhydrophilic and underwater superoleophobic properties and superoleophilic and underoil highly hydrophobic properties. Moreover, we propose an oil/water filtration device, which can be continuously operated, and the separation efficiency was recovered after backward extrusion. Quartz sand modified with coconut shell powder could also adsorb dyes.

2. Materials and Methods

2.1. Materials

Coconut shell waste was purchased from Hainan Wenchang Coconut Product Factory. Quartz sand (0.3–0.6 mm) was purchased from Henan Gongyi Hongda Filter Media Factory. Hexane, dichloromethane, trichloromethane, anhydrous ethanol, and petroleum ether were purchased from Rionlon Bohua (Tianjin, China) Pharmaceutical and Chemical Co., Ltd, Tianjin, China. Heptane and methylene blue (MB) were sourced from Tianjin Damao Chemical Reagent Factory, Tianjin, China, AR. Cyclohexane was purchased from Taicang Hushi Reagent Co., Ltd., Shanghai, China; sodium hydroxide was from Tianjin BASF Chemical Co., Ltd., Tianjin, China; waterborne polyurethane (PU) was bought from Shenzhen Jitian Chemical Co., Ltd., Shenzhen, China; engine oil was purchased from Beijing Kunlun Lubricating Oil Factory, Beijing, China. Diesel oil was bought from a local gas station, rapeseed oil was bought from a local oil mill, and distilled water was prepared in the laboratory.

2.2. Characterization of Filter Media

Static contact angle was measured using an optical contact angle measuring instrument (OCA25, Eastern-Dataphy, Germany). Quartz sand was tiled on a glass slide and then placed in a quartz glass dish containing water (or oil). Then, 3 μL of oil (or water) was dripped. The contact angle of underwater oil (or underoil water) was measured 15 s later at three different positions, and the average value was calculated. The surface morphology of the filter media was characterized using a low-vacuum scanning electron microscope (SEM, JSM-5600LV, JEOL, Tokyo, Japan). The chemical structure of the filter media was analyzed using an infrared spectrometer (FTIR, VERTEX 70, Bruker, Karlsruhe, Germany). The elements on the surface of the filter media were analyzed by a multi-functional electronic energy spectrometer (XPS, PHI-5702, Physical Electronic, Inc., Chanhassen, MN, USA).

2.3. Preparation of Quartz Sand Filter Media with Special Wettability

Coconut shell was washed with distilled water, dried in an oven at 105 °C for 24 h, and ground with a grinder to a particle size of 400 mesh. Coconut shell powder (20 g) was mixed with 100 mL of 0.1 mol/L NaOH with stirring for 4 h using a magnetic stirrer (S10-2, Sile Instrument Co., Ltd., Shanghai, China). Then, the mixture was ultrasonically dispersed using an ultrasonic cleaner (KQ5200DB, Kunshan Ultrasonic Instrument Co., Ltd., Kunshan, China) for 2 h at 60 kHz and separated through centrifugation. The mixture was washed with deionized water until the pH of the solution was 7. Finally, the solution was dried in an oven at 60 °C to obtain the activated coconut shell powder. Activated coconut shell powder (12.5 g) was dispersed in 500 mL of anhydrous alcohol and added with 2.5 g waterborne PU with magnetic stirring for 2 h to obtain uniform dipping solution. The quartz sand was immersed into the dipping solution for 48 h, then screened out, and dried in an oven at 60 °C for 48 h. The quartz sand filter media coated with coconut shell powder (hereinafter referred to as CSQS) with superhydrophilic and underwater superoleophobic properties and superoleophilic and underoil highly hydrophobic properties was obtained.

2.4. Oil/Water Separation Device and Experimental Method

The oil/water separation device consisted of a T-shaped glass tube with a length of 20 cm and an inner diameter of 3 cm in the middle and a glass filter column with a length of 10 cm and an inner diameter of 3 cm on both sides as shown in Figure 1. The interface was connected by a flange and fixed with screws. A 200-mesh stainless steel mesh was sandwiched in the middle of the flange to intercept and fix the quartz sand filter media. The two filter columns were filled with the same amount of CSQS filter media.

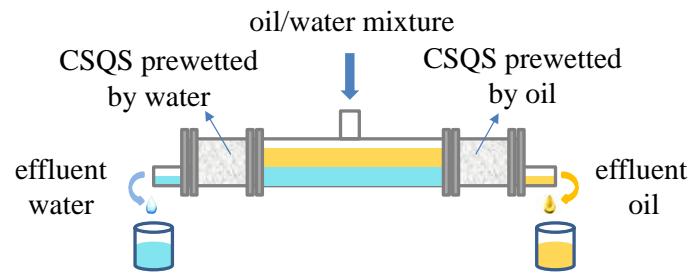


Figure 1. Diagram of the filtration experiment device.

The two filter columns were separately pre-wetted with oil and water. The filter column pre-wetted by water had superhydrophilic and underwater superoleophobic properties, whereas the filter column pre-wetted by oil had superoleophilic and underoil highly hydrophobic properties. The oil/water mixture (50% *v:v*) was poured in through the upper mouth of the T-shaped glass tube. Oil and water were stratified under the action of gravity. The liquid with low density was on the top, and the liquid with high density was at the bottom. The water phase flowed out from the superhydrophilic and underwater superoleophobic filter column whereas the oil phase flowed out from the superoleophilic and underoil highly hydrophobic filter column because of the selective filtration of the filter media. As a result, oil/water separation was achieved. The average values of three groups of parallel experiments were taken in all experiments.

The oil content in the filtered water was determined by a total carbon and total nitrogen analyzer (multi N/C 2100, Analytik Jena, Jena, Germany). The water content in the filtered oil was determined by a moisture meter for water content (SN-WS200A, Qingdao Sunde Environmental Protection Technology Co., Ltd., Qingdao, China). Separation efficiency was calculated based on the following formula:

$$\eta_{\text{water}} = \frac{C_{\text{O}_i} - C_{\text{O}_e}}{C_{\text{O}_i}} \times 100\% \quad (1)$$

$$\eta_{\text{oil}} = \frac{C_{\text{W}_i} - C_{\text{W}_e}}{C_{\text{W}_i}} \times 100\% \quad (2)$$

where η_{water} and η_{oil} refer to the oil separation efficiency of the water filter and the water separation efficiency of the oil filter, respectively; C_{O_i} and C_{W_i} refer to the initial oil and initial water contents of the oil/water mixture, respectively, in milligrams per liter; C_{O_e} and C_{W_e} refer to the oil content in effluent water and water content in effluent oil, respectively, in milligrams per liter.

Water (or oil) was removed from the superoleophilic (or superhydrophilic) side through backward extrusion after the continuously filtered diesel oil/water mixture was penetrated by lyophobic liquid. The device was operated as follows: super hydrophilic liquid was poured in from the liquid outlet, and lyophobic liquid was extruded with a certain pressure and poured out from the liquid inlet. The operation was repeated three times until the lyophobic liquid could not be observed in the liquid poured for filtration.

The permeability coefficients of the filter columns on the superoleophilic and superhydrophilic sides were calculated as follows:

$$K = \frac{Q \cdot L}{A \cdot \Delta h} \quad (3)$$

where K refers to permeability coefficient in meters per hour; Q refers to the seepage discharge per unit time in cubic meters per hour; L refers to the length of the column in meters; A refers to the cross-section area of water in square meters; Δh refers to the head loss of the filter layer in meters.

The intrusion pressure of lyophobic liquid was determined using the device shown in Figure 2. Taking the intrusion pressure of water as an example, 6-cm thick CSQS was filled in a glass tube with an inner diameter of 1.2 cm. Then, oil was used for pre-wetting. The height of the lifting table was adjusted to make the upper surface of the filter media layer in the glass tube to be equally high to the oil surface in the outer container. The purpose was to keep the oil static pressure inside and outside

the glass tube the same. A rubber dropper was used to slowly add water from the top of the glass tube (stained with MB for easy observation) until the water column just penetrated the surface of the CSQS. Blue liquid infiltration was observed in the filter layer. At this moment, the height difference between the water level and the surface of the filter layer in the glass tube was the intrusion height h_{\max} . The average value of three replicates was calculated. Water was exchanged with oil to measure the intrusion pressure of oil. Intrusion pressure was calculated based on the following formula:

$$P = \rho g h_{\max} \quad (4)$$

where P refers to intrusion pressure value in pascals; ρ refers to the density of invading liquid in kilograms per cubic meter; g refers to the gravitational acceleration in meters per square second; h_{\max} refers to the maximum height of invading liquid that the filter media can bear in meters.

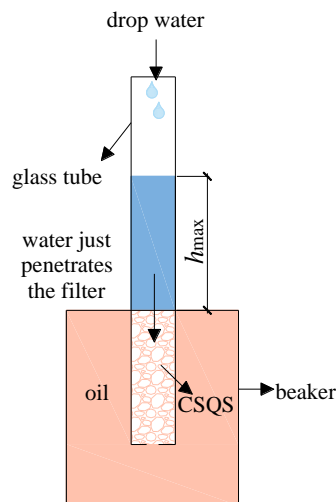


Figure 2. Diagram for water intrusion pressure device.

2.5. Dye Adsorption Experiment

MB (1 g) was dissolved in 1000 mL of distilled water to prepare MB stock solution with a concentration of 1000 mg/L. The stock solution was diluted with distilled water to the desired concentration for adsorption study. The adsorption experiment was performed as follows. A certain mass of CSQS was added into a 45-mL centrifuge tube containing 30 mL of MB solution. The centrifuge tube was placed in a vapor-bathing constant temperature vibrator (THZ-82A, Jintan Danyangmen Quartz Glass Factory, Changzhou, China) and shaken at 170 r/min for a certain time at 25 °C to obtain the supernatant. MB concentration was measured at $\lambda = 665$ nm using a UV spectrophotometer (UV-1800, Shanghai Mapada Instrument Co., Ltd., Shanghai, China). Then, the removal rate and adsorption capacity were calculated. The formulas are as follows:

$$\eta_{\text{MB}} = \frac{C_i - C_t}{C_i} \times 100\% \quad (5)$$

$$q_e = \frac{C_i - C_e}{m} V \quad (6)$$

where η_{MB} refers to the removal rate of MB; C_i and C_e refer to the initial and equilibrium concentrations of MB, respectively, C_t refers to the concentrations of MB after adsorption, in milligrams per liter; q_e refers to adsorption capacity in milligrams per gram; V refers to the volume of MB solution in liters; m refers to the mass of CSQS in grams.

2.6. Study on Wetting Stability

CSQS was immersed in four beakers that contain ethanol solution, which were placed in an ultrasonic cleaner and vibrated continuously at 60 kHz for 12, 24, 36, and 48 h. CSQS was taken out to dry in an oven at 60 °C. Then, the contact angles of underwater oil (UWOCA) and underoil water (UOWCA) were determined. The mechanical wear resistance of the filter media was analyzed. CSQS was immersed in the aqueous solution at pH 1, 5, 7, 11, and 14 for 24 h and taken out to dry in an oven at 60 °C. Then, the mechanical wear resistance of the quartz sand was measured. CSQS was immersed in an aqueous solution of surfactant sodium dodecyl benzene sulfonate (SDBS) for 48 h, taken out, rinsed repeatedly with deionized water, and dried. The properties of the CSQS resistant to surfactants were studied. CSQS was placed in air for 3 months, and its UWOCA and UOWCA were measured every other month to study its air exposure resistance.

3. Result and Discussion

3.1. Modified Mechanism

Coconut shell is composed of cellulose, hemicellulose, and lignin. The molecular formula of the cellulose is shown in Figure 3 [37]. Alkali activation can be used to reduce the crystallinity of cellulose, lessen the force of the hydrogen bonds, and expose a large number of hydroxyl groups to improve the solubility of cellulose. The $-\text{CH}_2\text{OH}$ group of activated cellulose will form a condensation reaction with the $-\text{OH}$ of quartz sand to graft the hydrophilic group onto the surface of quartz sand as shown in Figure 3. The addition of waterborne PU makes the cellulose combine with quartz sand more firmly and increases the roughness.

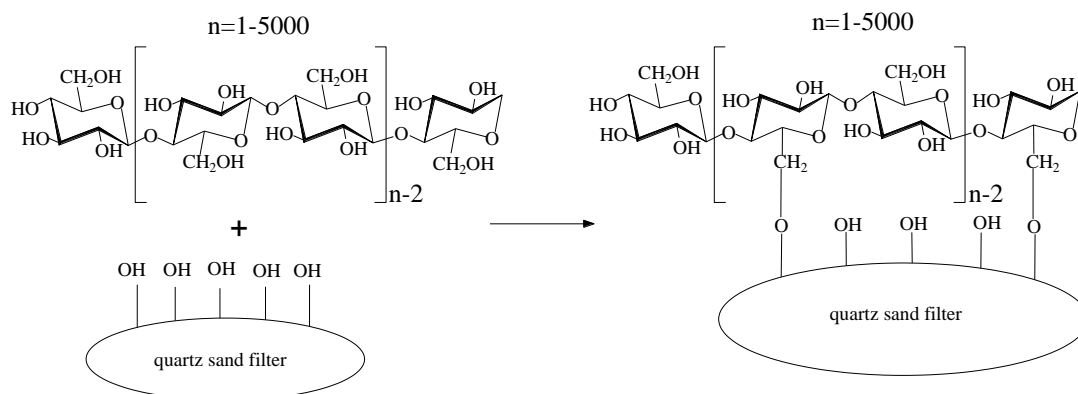


Figure 3. Schematic diagram of preparing make coconut shell powder-covered quartz sand filter media (CSQS).

3.2. Surface Wettability

In air, CSQS can be quickly wetted by water or oil, and the contact angles are 0° as shown in Figure 4a–c. This occurrence is due to the combined action of amphiphilic groups, such as hydroxyl and carboxyl groups, with the rough microstructure on the surface of CSQS. Water will be trapped after CSQS is immersed into water to form a layer of water film in the rough structure to prevent oil and grease from wetting the surface, which is underwater superoleophobic. The UWOCA of hexane, diesel oil, heptane, engine oil, rapeseed oil, petroleum ether, dichloroethane, and trichloromethane were more than 150° and reached the underwater superoleophobic level as shown in Figure 4d–f. Similarly, CSQS was first immersed in oil and formed a layer of oil film on the surface of quartz sand in advance to reduce the contact area between water droplet and the surface of quartz sand. The UOWCAs of different oils were within the range of 130–150° and reached the underoil highly hydrophobic level.

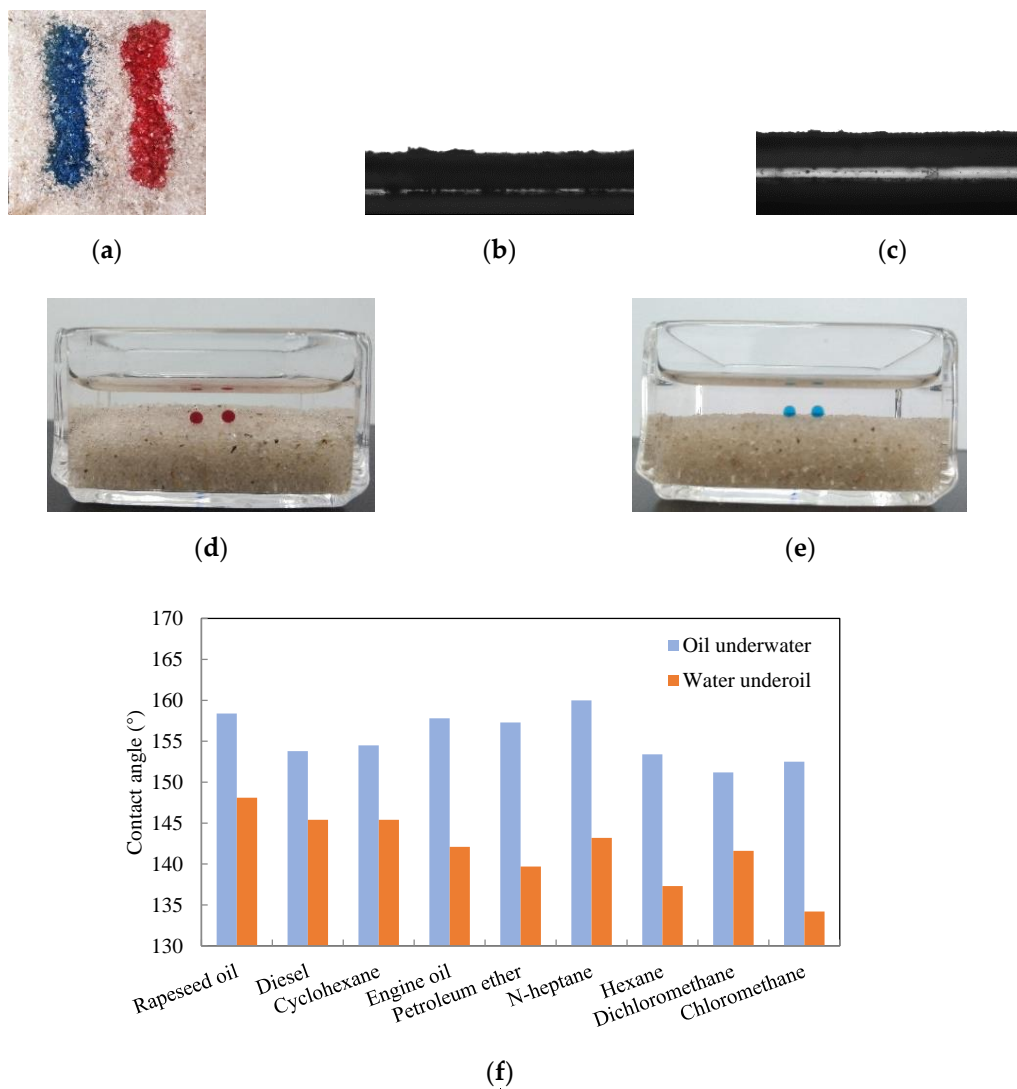


Figure 4. The contact angle of CSQS. (a) Water droplets (colored blue by methylene blue) and oil droplets (colored red by oil red O) on the CSQS surface in air, respectively; (b) the water contact angle is 0° ; (c) the oil contact angle is 0° ; (d) contact angle picture of dichloromethane underwater on CSQS surface; (e) contact angle picture of water under cyclohexane on CSQS surface; (f) contact angles of water under oils and oils under water.

3.3. SEM Analysis

The SEM images of unmodified quartz sand and CSQS are shown in Figure 5. The original quartz sand was made by external grinding and crushing; thus, it presents irregular section and edge angle with a smooth surface. The surface of CSQS had patch and strip-shaped fine particles, which belong to coconut shell powder particles with rough micro/nanostructure and undeveloped surface porosity.

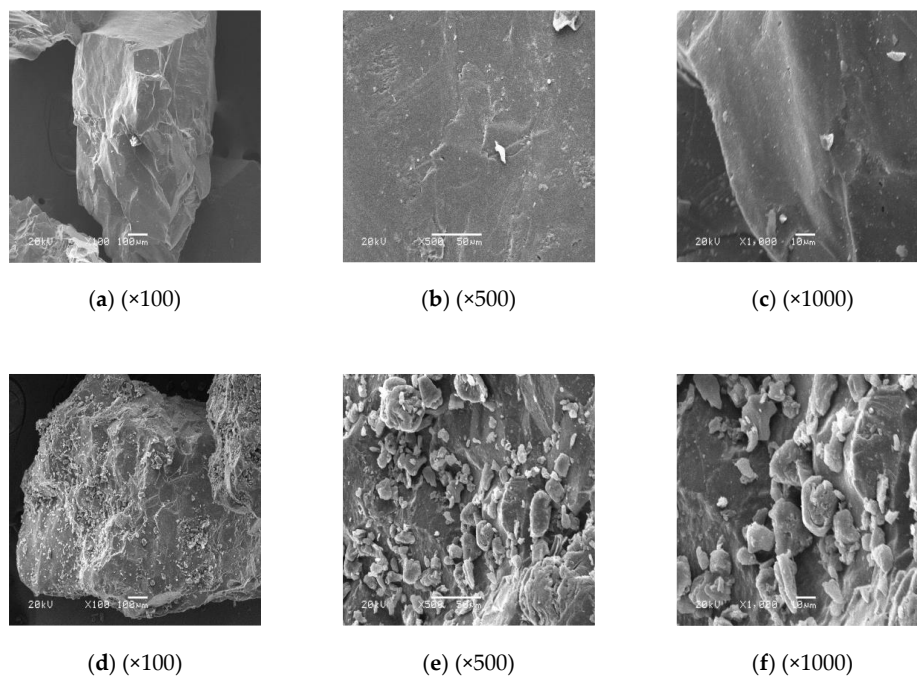


Figure 5. SEM images of (a–c) unmodified quartz sand; (d–f) CSQS.

3.4. FTIR Analysis

The infrared spectrum analysis of quartz sand was carried out as shown in Figure 6 to confirm the changes in the surface functional groups of quartz sand before and after modification with coconut shell powder. A strong absorption peak is present near 3464/cm, which is the stretching vibration peak of the –OH group from cellulose, hemicellulose, monosaccharide, and polysaccharide. CSQS has a slightly enhanced adsorption strength and thus more easily absorbs water compared with the unmodified quartz sand. A new absorption peak appeared in the infrared spectrum of the modified quartz sand. The absorption peak in 1300–1000/cm is the C–O stretching vibration peak. The small and sharp absorption peak in 1450/cm is the stretching vibration peak of benzene ring skeleton with C=C group. A stretching vibration that belongs to the C=O group appeared in 1850–1600/cm. This finding indicates that coconut shell powder adhered on the surface of quartz sand successfully. In conclusion, coconut shell powder was introduced on the surface of quartz sand, and more hydrophilic polar groups, such as hydroxyl and carboxyl groups, were introduced. The two amphiphilic groups play a key role in the preparation of the superhydrophilic and underwater superoleophobic surface and the superoleophilic and underoil highly hydrophobic surface.

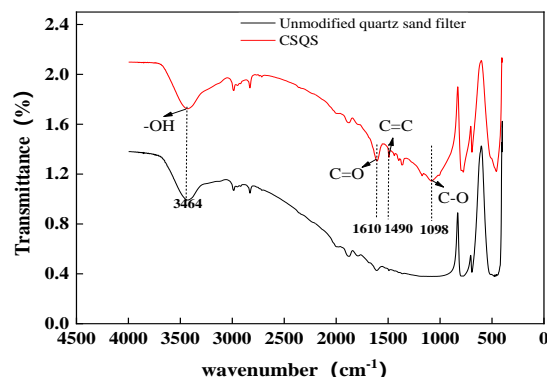


Figure 6. FTIR spectra of CSQS.

3.5. XPS Analysis

XPS analysis was performed to analyze the changes in the elements on the surface of quartz sand before and after modification as shown in Figure 7. Four groups of characteristic peaks with obvious strength, namely, O1s, C1s, Si2s, and Si2p, were detected in quartz sand before and after modification. The surface of quartz sand is composed of Si and O. The comparative result shows that C1s absorption peak in 295 eV was obviously enhanced and the number of C elements increased in the CSQS energy spectrum. The additional C came from the main components of the coconut shell and indicated that coconut shell powder was bound to the surface of quartz sand [36]. The characteristic peaks in O1s, Si2s, and Si2p were slightly weakened because of the coconut shell powder covering. A weak N1s characteristic peak appeared in 398.4 eV, which indicated that the adhesive waterborne PU attached to the quartz sand.

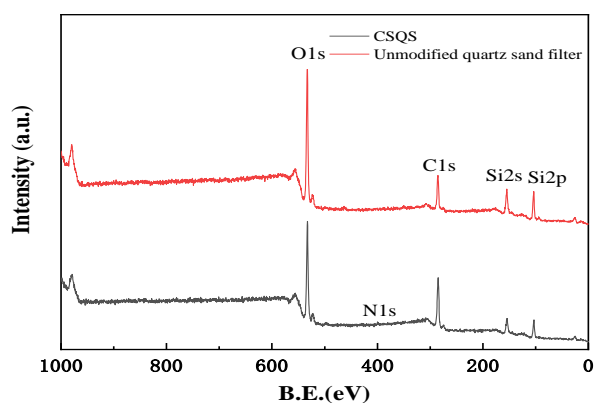


Figure 7. XPS spectra of CSQS.

3.6. Oil/Water Separation Performance

Figure 8 shows the continuous separation of the diesel oil/water mixture, and Figure 8a shows a photo of the device. The left filter column contained the superhydrophilic and underwater superoleophobic quartz sand, and the right filter column contained the superoleophilic and underoil highly hydrophobic quartz sand. The separation efficiencies of diesel oil, cyclohexane, engine oil, petroleum ether, rapeseed oil, dichloromethane, trichloromethane, and water mixture are shown in Figures 8b and 9a. The oil separation efficiency of filtered water was more than 99.99%, and the water separation efficiency of filtered oil was more than 99.92%; thus, the separation efficiency of the device is very good. The continuous separation efficiency of diesel/water mixture is shown in Figure 9b. The efficiency is still more than 99.99% after separating 7.1 L of the mixture. Afterward, the filtered water gradually penetrated into the oil part as shown in Figure 8c. This penetration led to a sudden decrease in oil separation efficiency as shown in Figure 9b at 7.7 L. At this moment, the oil phase was discharged from the pores of the filter media by reverse extrusion (Section 2.4), and filtration was continued. The oil removal efficiency was restored to 99.99% above. Oil penetration appeared for the second time on the superhydrophilic side when 10.8 L of oil/water mixture was separated. The separation was continued after reverse extrusion. The efficiency was restored to 99.99% again. In this experiment, 12.3 L of mixture was continuously separated. The superhydrophilic side was not penetrated again, whereas the superoleophilic side was never penetrated. The oil/water separation lasted for 24.6 h, and the average filtration rate of oil and water was 0.5 L/h. Therefore, the continuous filtration device can be used to continuously and efficiently separate oil/water mixture.

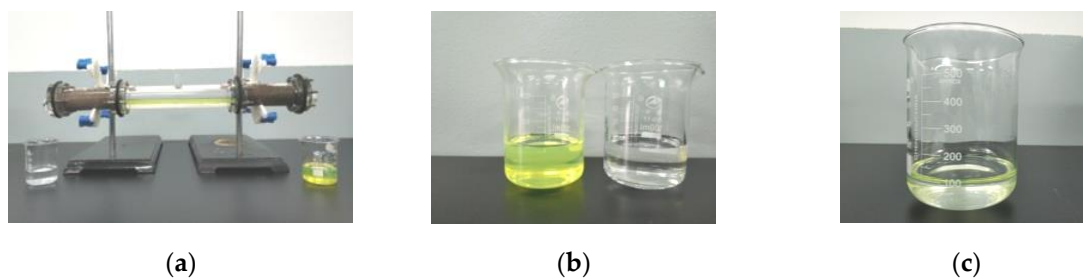


Figure 8. Experimental diagram of filtering oil/water mixture. (a) Continuous oil/water separation device filters the mixture of diesel and water; (b) oil and water after filtration; (c) penetration on the water outlet side and filter out the oil.

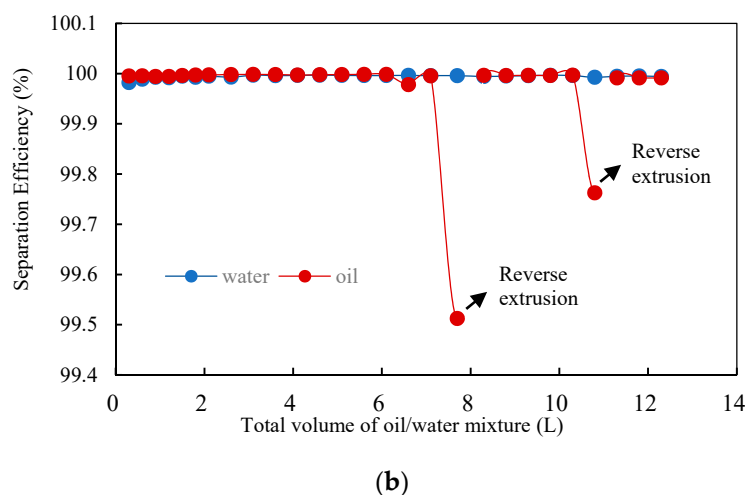
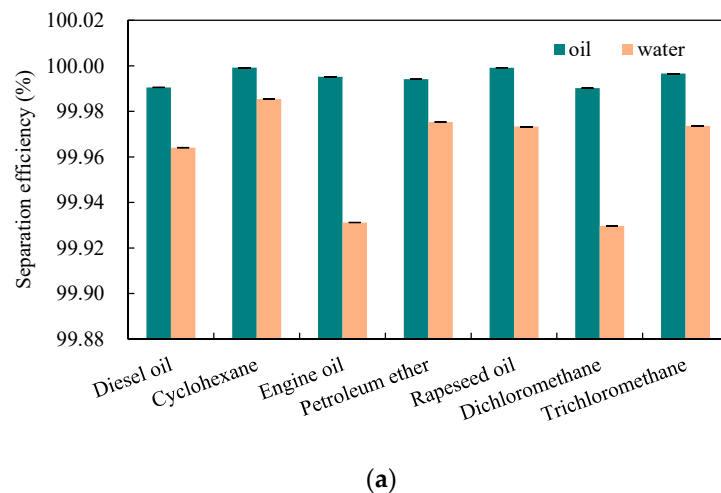


Figure 9. Separation efficiency of oil/water mixture. (a) Separation efficiency of different kinds of oil/water mixture; (b) separation efficiency of diesel and water mixture filtered continuously.

Figure 10 shows the permeability coefficients of oil and water when separating different types of oil/water mixtures by a continuous separation device. Permeability coefficient is used for measuring separation speed. Permeability coefficient is related to the type, viscosity, and density of oil. Table 1 lists the viscosity, density, and other characteristics of the seven kinds of oil used in the experiment. The data is viewed on the packaging of experimental drugs. The densities of dichloromethane and trichloromethane are higher than that of water, whereas the densities of the five other oils are lower than that of water. Engine oil, rapeseed oil, and diesel oil have high viscosity; therefore, the filter column on the oleophilic side produced oil slowly, and their permeability coefficients were 2.71, 0.13, and 1.35 m/h,

respectively. The permeability coefficients of the other oils were high. The permeability coefficient of cyclohexane was 4.74 m/h, and those of petroleum ether, dichloromethane, and trichloromethane were higher than 10 m/h. The permeability coefficient of water reached 9.37 m/h. Generally, the device has a faster separation speed for oil with lower viscosity.

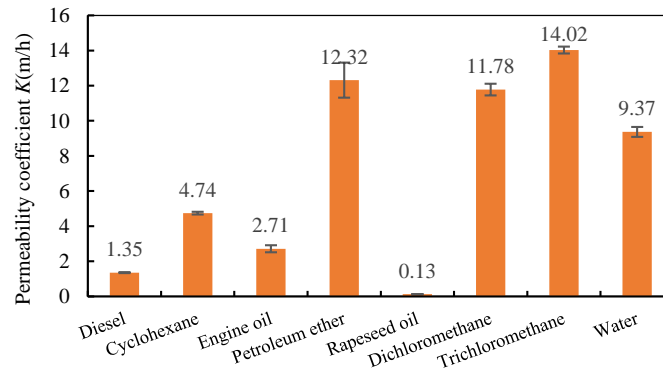


Figure 10. The permeability coefficients of the water outlet and oil outlet when filtering different oils.

Table 1. Types and characteristics of oil.

| Characteristic | Density (g/mL) | Viscosity (mPa·s) |
|------------------|----------------|--------------------|
| Water | 1 | 1×10^{-9} |
| Diesel oil | 0.81–0.855 | 2.87 |
| Cyclohexane | 0.779 | 1 |
| Engine oil | 0.88~0.89 | 105.4 |
| Petroleum ether | 0.64–0.66 | 0.3 |
| Rapeseed oil | 0.923 | 12.5–12.9 |
| Dichloromethane | 1.325 | 0.429 |
| Trichloromethane | 1.484 | 0.563 |

The measured intrusion pressure of CSQS is shown in Figure 11. A larger intrusion pressure indicates that a larger pressure is required to make lyophobic liquid (water or oil) pass through the surface; thus, the device is more stable. The intrusion pressures of underoil and underwater are the intrusion pressures on the superhydrophilic and superoleophilic sides, respectively. Figure 11 shows that the value on the superoleophilic side is larger than that on the superhydrophilic side. This difference is also the reason why the superhydrophilic side was penetrated.

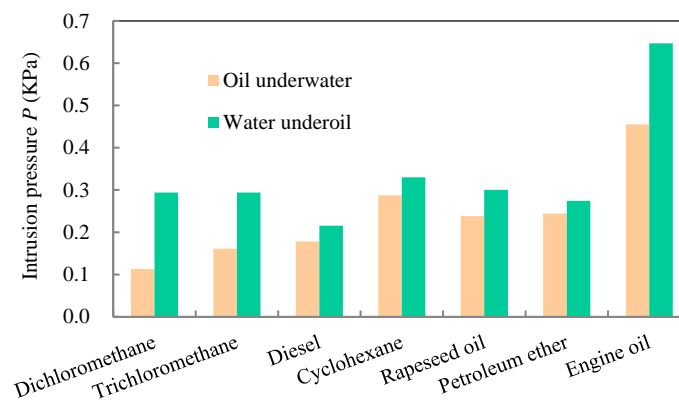


Figure 11. Intrusion pressure of CSQS.

Figure 12 shows the capillary pressure diagram of the superhydrophilic and underwater superoleophobic filter media and the underoil superhydrophobic filter media. According to Laplace theory, the theoretical intrusion pressure formula is:

$$\Delta P = \frac{2\gamma}{R} = \frac{-l\gamma \cos \theta_a}{A} \quad (7)$$

where ΔP refers to the theoretical intrusion pressure in pascals; γ refers to the surface tension of liquid in milliNewtons per meter; R refers to the curvature radius in meters; l refers to mesh perimeter in meters; θ_a refers to the contact angle of liquid on the prepared surface in degrees; A refers to the cross-section area of the mesh in square meters.

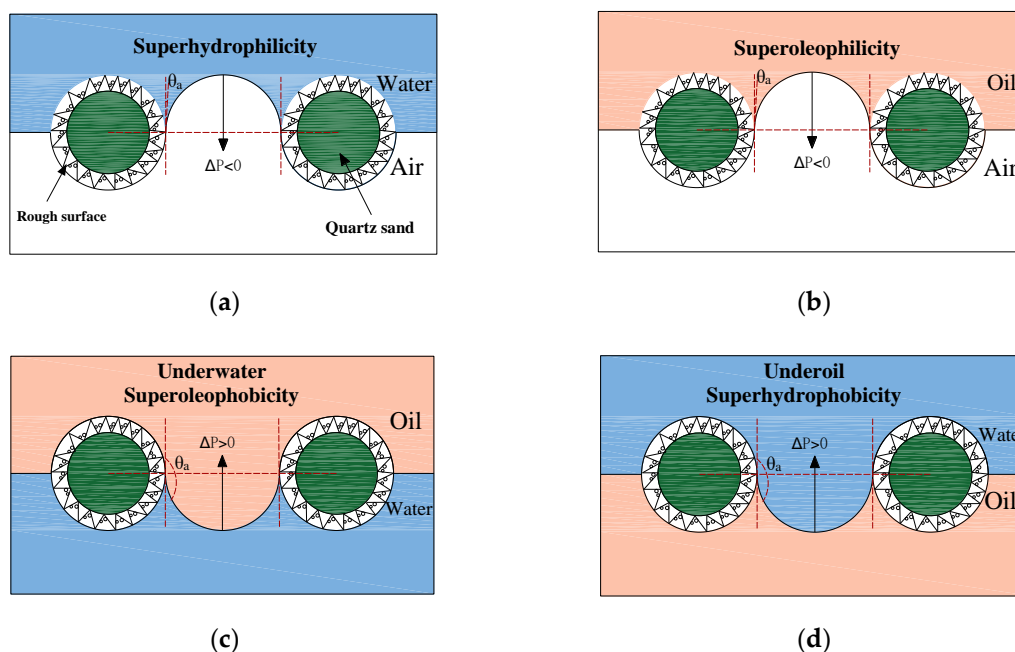


Figure 12. Theoretical wetting model of superhydrophilic and underwater superoleophobic or superoleophilic and underoil superhydrophobic filter media. (a) In air, water can pass through superhydrophilic quartz sand; (b) in air, oil can pass through superoleophilic quartz sand; (c) underwater, oil cannot pass through underwater superhydrophobic quartz sand; (d) under oil, water cannot pass through underoil superhydrophobic quartz sand.

The oil phase and water phase flowed out from the superoleophilic and superhydrophilic outlets, respectively, under the action of capillary pressure and gravity when the oil/water mixture was poured into the filter column. In air, the water contact angle (WCA) of the superhydrophilic filter media was less than 90° , and the capillary pressure of water points to the outlet side and drives the water phase to pass through. The oil contact angle (OCA) of the superoleophilic filter media was also less than 90° , and the capillary pressure of oil also drives the oil phase to flow out from the gap in the filter media. However, the UWOCA (or UOWCA) of underwater superoleophobic surface (or underoil superhydrophobic surface) is greater than 90° under water (or under oil). Therefore, ΔP is more than 0, and the capillary pressure of oil (or water) points to the inlet side to prevent the oil phase (or water phase) from passing through the filter media to effectively separate the oil/water mixture. In addition, this device can be used to solve problems in liquid accumulation and oil density limitation.

3.7. Adsorbed Dyes

In this paper, the adsorption effects of unmodified quartz sand and CSQS on MB were compared. The removal rates of the unmodified quartz sand and CSQS were 10.7% and 87.81%, respectively,

when the initial concentration was 200 mg/L, the dose of quartz sand was 20 g, and the adsorption time was 60 min. This result indicates that the adsorption effect of unmodified quartz sand on MB is poor, whereas that of CSQS is greatly improved. Figure 13 shows the experimental results of the static adsorption of MB by CSQS. The concentration of MB in the supernatant decreased from 158.72 to 2.35 mg/L and the removal rate increased from 20.64% to 98.83% as CSQS increased from 5 to 40 g when the initial MB concentration was 200 mg/L and the contact time was 1 h. This result indicates that CSQS has a strong ability of adsorbing and removing MB. The removal rate increased rapidly with the increase in mass when CSQS was less than 20 g, but the rising trend obviously slowed down and tended to be stable when CSQS was more than 20 g. Therefore, the optimal dose of CSQS was 20 g. Removal efficiency increases with the increase in dosage because of the availability of the adsorbent in more active sites. The dye adsorption capacity increased rapidly within 15 min and the MB removal rate reached 71.97% when the initial MB concentration was 200 mg/L and CSQS was 20 g. Afterward, dye adsorption slowed down and reached the balance within 60 min. The maximum removal rate was 87.81%, and the adsorption capacity was 0.26 mg/g. The reason is that many adsorption sites were available on the surface of CSQS at the beginning of the adsorption; thus, MB was adsorbed immediately upon contact with CSQS. The adsorption capacity of CSQS gradually decreased and reached the adsorption equilibrium with the increase in adsorption time. The MB removal rate decreased from 98.94% to 86.16%, and the adsorption capacity increased from 0.04 to 0.26 mg/g when CSQS was 20 g, the reaction time was 1 h, and the initial MB concentration of MB increased from 25 to 200 mg/L. Adsorption power and adsorption capacity are driven to increase with the initial concentration if the concentration difference is large. Therefore, CSQS can effectively adsorb MB in a short time and successfully separate water-soluble cationic dyes.

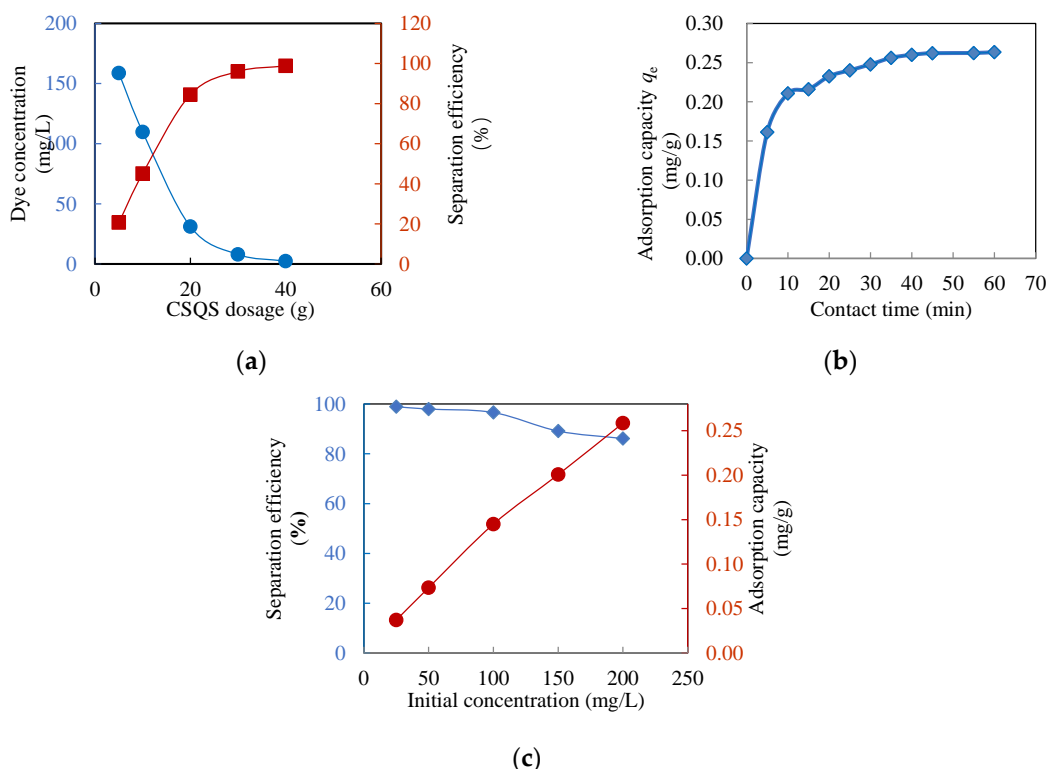


Figure 13. The effect of CSQS dosage, contact time, and initial concentration on the adsorption of methylene blue (MB). (a) The influence of quartz sand dosage on the concentration and separation efficiency after adsorption. The initial concentration is 200 mg/L and the contact time is 1 h. (b) The influence of contact time on the adsorption capacity of quartz sand. The initial concentration is 200 mg/L and CSQS dosage is 20 g. (c) The effect of initial concentration on MB removal rate and adsorption capacity. The CSQS dosage is 20 g and the oscillation time is 1 h.

3.8. Stability Study

Stability is an important factor for the application of super wettable materials. Figure 14 shows the stability of CSQS. Ultrasonic treatment is often used to clean substances but can physically destroy the surface that is not chemically bonded to the substrate. Therefore, ultrasonic oscillation can be used to measure the mechanical wear properties of quartz sand [38]. Figure 14 shows that the WCA of quartz sand immersed in cyclohexane was kept at 145.4° after ultrasonic oscillation for 12 h. WCA decreased by 1.3° after 24 h of oscillation and became stable afterward. The contact angle of dichloromethane in water slightly decreased after 48 h of ultrasonic treatment and remained at 138.8° . The contact angles of underwater cyclohexane and underwater dichloromethane remained at 154.1° and 151.1° , respectively, after 48 h of ultrasonic treatment. This result shows underwater superoleophobic property and indicates that CSQS has strong mechanical wear resistance. UWOCA and UOWCA were unchanged after being soaked and washed with SDBS. CSQS remains stable in surfactant solutions; thus, it can be washed with surfactant after being contaminated by oil and can also be used to separate the emulsion with stable surfactant. The contact angles of underwater dichloromethane and dichloromethane in water slightly decreased in acidic environment (pH 1 and 5) and remained stable in other pH conditions. (pH 7, 11, and 14). Therefore, CSQS has strong acid–base resistance. The contact angle of CSQS remained stable after being placed in air for 3 months. Hence, CSQS is suitable for long-term storage. The studies show that CSQS has a strong ability to resist harsh environments.

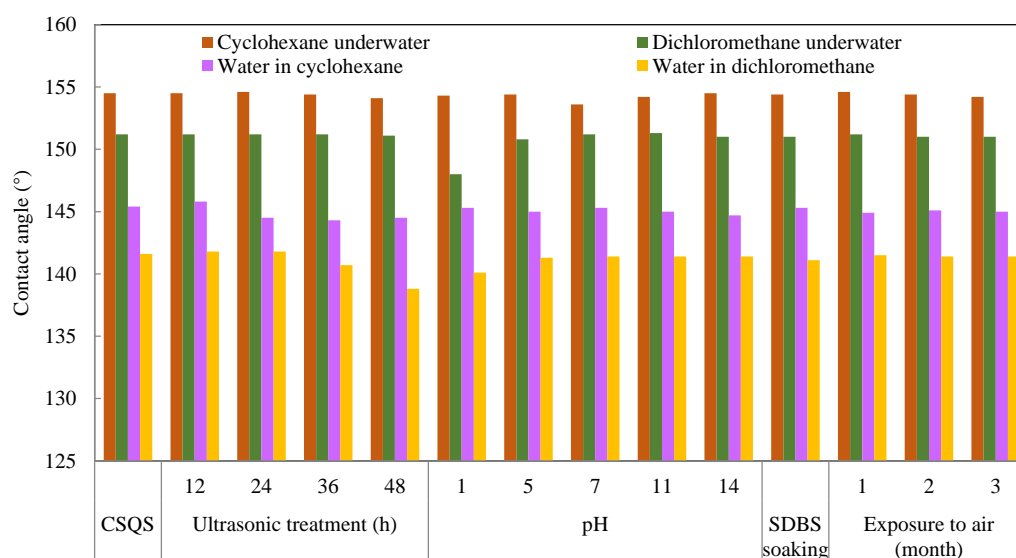


Figure 14. The contact angle of CSQS after ultrasonic treatment, sodium dodecylbenzene sulfonate cleaning, soaking.

4. Conclusions

We successfully prepared quartz sand filter media modified by coconut shell powder with superhydrophilic and underwater superoleophobic properties and superoleophilic and underoil highly hydrophobic properties by simple dip-coating method. WCA and OCA were about 0° . UWOCA and UOWCA were as high as 151.2° and 134.2° , respectively. FTIR, SEM, and XPS analyses showed that coconut shell powder was successfully grafted onto the surface of quartz sand. The designed continuous oil/water separation device has a good separation effect on oil (heavy/light oil)/water mixture. The oil and water separation efficiencies were more than 99.99% and 99.92%, respectively. CSQS has good continuous separation performance. The lyophobic liquid can be discharged through backward extrusion even after penetration, and the separation efficiency can be recovered to 99.99%. The amphiphilic groups of CSQS have strong adsorption properties for dyes. The MB removal rate was as high as 98.94%. A series of physical and chemical tests proved that the CSQS has excellent corrosion

resistance, mechanical durability, and environmental durability. CSQS can separate oil/water mixture continuously and efficiently. At the same time, CSQS can effectively adsorb dyes in wastewater; thus, CSQS has a certain industrial applicability. Biomass material is cheap, easy to handle, and has more advantages compared with special wettable materials modified by other chemicals; thus, CSQS can be widely used in oil/water separation and dye adsorption.

Author Contributions: Conceptualization, B.W.; methodology, X.L.; investigation, X.L., X.S., H.G., G.W. and H.Z.; writing—original draft preparation, X.L.; writing—review and editing, B.W.; visualization, L.D.; supervision, L.D.; project administration, X.S.; funding acquisition, B.W. All authors have read and agreed to the published version of the manuscript.

Funding: This research was funded by National Natural Science Foundation of China (No. 51668032) and the foundation of a Hundred Youth Talents Training Program of Lanzhou Jiaotong University (No. 152022).

Conflicts of Interest: The authors declare no conflict of interest.

References

1. Jiang, J.; Zhang, Q.; Zhan, X.; Chen, F. A multifunctional gelatin-based aerogel with superior pollutants adsorption, oil/water separation and photocatalytic properties. *Chem. Eng. J.* **2019**, *358*, 1539–1551. [[CrossRef](#)]
2. Rosell-Mele, A.; Moraleda-Cibrian, N.; Cartro-Sabate, M.; Colomer-Ventura, F.; Mayor, P.; Orta-Martinez, M. Oil pollution in soils and sediments from the Northern Peruvian Amazon. *Sci. Total Environ.* **2018**, *610*, 1010–1019. [[CrossRef](#)] [[PubMed](#)]
3. Raymond, T.; King, C.K.; Raymond, B.; Stark, J.S.; Snape, I. Oil Pollution in Antarctica. In *Oil Spill Science and Technology*, 2nd ed.; Elsevier: Cambridge, MA, USA, 2017; pp. 759–803.
4. Alshavef, M.S.; Javed, A. Assessment of Relative Tectonics Activity Zones in Masila Oil Field, Yemen. *JGSA* **2020**, *4*, 16.
5. Abed, R.M.M.; Al-Kindi, S. Effect of disturbance by oil pollution on the diversity and activity of bacterial communities in biological soil crusts from the Sultanate of Oman. *Appl. Soil Ecol.* **2017**, *110*, 88–96. [[CrossRef](#)]
6. Fox, C.H.; O'Hara, P.D.; Bertazzon, S.; Morgan, K.; Underwood, F.E.; Paquet, P.C. A preliminary spatial assessment of risk: Marine birds and chronic oil pollution on Canada's Pacific coast. *Sci. Total Environ.* **2016**, *573*, 799–809. [[CrossRef](#)]
7. Chequer, F.M.; Lizier, T.M.; de Felicio, R.; Zanoni, M.V.; Deboni, H.M.; Lopes, N.P.; de Oliveira, D.P. The azo dye Disperse Red 13 and its oxidation and reduction products showed mutagenic potential. *Toxicol. Vitr.* **2015**, *29*, 1906–1915. [[CrossRef](#)]
8. Bruschweiler, B.J.; Merlot, C. Azo dyes in clothing textiles can be cleaved into a series of mutagenic aromatic amines which are not regulated yet. *Regul. Toxicol. Pharm.* **2017**, *88*, 214–226. [[CrossRef](#)] [[PubMed](#)]
9. Shamaei, L.; Khorshidi, B.; Perdicakis, B.; Sadrzadeh, M. Treatment of oil sands produced water using combined electrocoagulation and chemical coagulation techniques. *Sci. Total Environ.* **2018**, *645*, 560–572. [[CrossRef](#)] [[PubMed](#)]
10. Nampoothiri, M.G.H.; Manilal, A.M.; Soloman, P.A. Control of Electrocoagulation batch reactor for oil removal from automobile garage wastewater. *Procedia Technol.* **2016**, *24*, 603–610. [[CrossRef](#)]
11. Zhao, L.; Li, R.; Xu, R.; Si, D.; Shang, Y.; Ye, H.; Zhang, Y.; Ye, H.; Xin, Q. Antifouling slippery liquid-infused membrane for separation of water-in-oil emulsions. *J. Membr. Sci.* **2020**, *611*, 118289. [[CrossRef](#)]
12. Sun, Y.; Guo, Z. Novel and cutting-edge applications for a solvent-responsive superoleophobic–superhydrophilic surface: Water-infused omniphobic surface and separating organic liquid mixtures. *Chem. Eng. J.* **2020**, *381*, 122629. [[CrossRef](#)]
13. Yang, J.; Wang, L.; Xie, A.; Dai, X.; Yan, Y.; Dai, J. Facile surface coating of metal-tannin complex onto PVDF membrane with underwater Superoleophobicity for oil-water emulsion separation. *Surf. Coat. Technol.* **2020**, *389*, 125630. [[CrossRef](#)]
14. Yu, T.; Halouane, F.; Mathias, D.; Barras, A.; Wang, Z.; Lv, A.; Lu, S.; Xu, W.; Meziane, D.; Tiercelin, N.; et al. Preparation of magnetic, superhydrophobic/superoleophilic polyurethane sponge: Separation of oil/water mixture and demulsification. *Chem. Eng. J.* **2020**, *384*. [[CrossRef](#)]

15. Zou, L.; Phule, A.D.; Sun, Y.; Zhu, T.Y.; Wen, S.; Zhang, Z.X. Superhydrophobic and superoleophilic polyethylene aerogel coated natural rubber latex foam for oil-water separation application. *Polym. Test.* **2020**, *85*, 123339. [[CrossRef](#)]
16. Nine, M.J.; Kabiri, S.; Sumona, A.K.; Tung, T.T.; Moussa, M.M.; Losic, D. Superhydrophobic/superoleophilic natural fibres for continuous oil-water separation and interfacial dye-adsorption. *Sep. Purif. Technol.* **2020**, *233*, 116062. [[CrossRef](#)]
17. Priyanka, M.; Saravanakumar, M.P. Ultrahigh adsorption capacity of starch derived zinc based carbon foam for adsorption of toxic dyes and its preliminary investigation on oil-water separation. *J. Clean. Prod.* **2018**, *197*, 511–524. [[CrossRef](#)]
18. Yin, X.; Yu, S.; Wang, L.; Li, H.; Xiong, W. Design and preparation of superhydrophobic NiS nanorods on Ni mesh for oil-water separation. *Sep. Purif. Technol.* **2020**, *234*, 116126. [[CrossRef](#)]
19. Yue, X.; Li, Z.; Zhang, T.; Yang, D.; Qiu, F. Design and fabrication of superwetting fiber-based membranes for oil/water separation applications. *Chem. Eng. J.* **2019**, *364*, 292–309. [[CrossRef](#)]
20. Wang, B.; Liang, W.; Guo, Z.; Liu, W. Biomimetic super-lyophobic and super-lyophilic materials applied for oil/water separation: A new strategy beyond nature. *Chem. Soc. Rev.* **2015**, *44*, 336–361. [[CrossRef](#)]
21. Deng, Y.; Peng, C.; Dai, M.; Lin, D.; Ali, I.; Alhewairini, S.S.; Zheng, X.; Chen, G.; Li, J.; Naz, I. Recent development of super-wettable materials and their applications in oil-water separation. *J. Clean. Prod.* **2020**, *266*, 121624. [[CrossRef](#)]
22. Jiang, B.; Zhang, H.; Sun, Y.; Zhang, L.; Xu, L.; Hao, L.; Yang, H. Covalent layer-by-layer grafting (LBLG) functionalized superhydrophobic stainless steel mesh for oil/water separation. *Appl. Surf. Sci.* **2017**, *406*, 150–160. [[CrossRef](#)]
23. Cheng, Y.; Barras, A.; Lu, S.; Xu, W.; Szunerits, S.; Boukherroub, R. Fabrication of superhydrophobic/superoleophilic functionalized reduced graphene oxide/polydopamine/PFDT membrane for efficient oil/water separation. *Sep. Purif. Technol.* **2020**, *236*, 116240. [[CrossRef](#)]
24. Tang, W.; Sun, D.; Liu, S.; Li, B.; Sun, W.; Fu, J.; Li, B.; Hu, D.; Yu, J. One step electrochemical fabricating of the biomimetic graphene skins with superhydrophobicity and superoleophilicity for highly efficient oil-water separation. *Sep. Purif. Technol.* **2020**, *236*, 116293. [[CrossRef](#)]
25. Miao, W.; Jiao, D.; Wang, C.; Han, S.; Shen, Q.; Wang, J.; Han, X.; Hou, T.; Liu, J.; Zhang, Y. Ethanol-induced one-step fabrication of superhydrophobic-superoleophilic poly(vinylidene fluoride) membrane for efficient oil/water emulsions separation. *J. Water Process Eng.* **2020**, *34*, 101121. [[CrossRef](#)]
26. Wei, Y.; Xie, Z.; Qi, H. Superhydrophobic-superoleophilic SiC membranes with micro-nano hierarchical structures for high-efficient water-in-oil emulsion separation. *J. Membr. Sci.* **2020**, *601*, 117842. [[CrossRef](#)]
27. Jamalludin, M.R.; Hubadillah, S.K.; Harun, Z.; Othman, M.H.D.; Yunus, M.Z.; Ismail, A.F.; Salleh, W.N.W. Facile fabrication of superhydrophobic and superoleophilic green ceramic hollow fiber membrane derived from waste sugarcane bagasse ash for oil/water separation. *Arab. J. Chem.* **2020**, *13*, 3558–3570. [[CrossRef](#)]
28. Mi, H.-Y.; Jing, X.; Xie, H.; Huang, H.-X.; Turng, L.-S. Magnetically driven superhydrophobic silica sponge decorated with hierarchical cobalt nanoparticles for selective oil absorption and oil/water separation. *Chem. Eng. J.* **2018**, *337*, 541–551. [[CrossRef](#)]
29. Huang, A.; Kan, C.-C.; Lo, S.-C.; Chen, L.-H.; Su, D.-Y.; Soesanto, J.F.; Hsu, C.-C.; Tsai, F.-Y.; Tung, K.-L. Nanoarchitected design of porous ZnO@copper membranes enabled by atomic-layer-deposition for oil/water separation. *J. Membr. Sci.* **2019**, *582*, 120–131. [[CrossRef](#)]
30. Wang, X.; Xiao, C.; Liu, H.; Chen, M.; Xu, H.; Luo, W.; Zhang, F. Robust functionalization of underwater superoleophobic PVDF-HFP tubular nanofiber membranes and applications for continuous dye degradation and oil/water separation. *J. Membr. Sci.* **2020**, *596*, 117583. [[CrossRef](#)]
31. Li, X.; Shan, H.; Zhang, W.; Li, B. 3D printed robust superhydrophilic and underwater superoleophobic composite membrane for high efficient oil/water separation. *Sep. Purif. Technol.* **2020**, *237*, 116324. [[CrossRef](#)]
32. Yu, L.; Kanezashi, M.; Nagasawa, H.; Tsuru, T. Phase inversion/sintering-induced porous ceramic microsheet membranes for high-quality separation of oily wastewater. *J. Membr. Sci.* **2020**, *595*, 117477. [[CrossRef](#)]
33. Chen, C.; Wang, B.; Liu, H.; Chen, T.; Zhang, H.; Qiao, J. Synthesis of 3D dahlia-like Co₃O₄ and its application in superhydrophobic and oil-water separation. *Appl. Surf. Sci.* **2019**, *471*, 289–299. [[CrossRef](#)]
34. Li, J.; Long, Y.; Xu, C.; Tian, H.; Wu, Y.; Zha, F. Continuous, high-flux and efficient oil/water separation assisted by an integrated system with opposite wettability. *Appl. Surf. Sci.* **2018**, *433*, 374–380. [[CrossRef](#)]

35. Xie, A.; Cui, J.; Chen, Y.; Lang, J.; Li, C.; Yan, Y.; Dai, J. Capillarity-driven both light and heavy oil/water separation via combined system of opposite superwetting meshes. *Sep. Purif. Technol.* **2019**, *215*, 1–9. [[CrossRef](#)]
36. Yanyan, L.; Kurniawan, T.A.; Zhu, M.; Ouyang, T.; Avtar, R.; Dzarfan Othman, M.H.; Mohammad, B.T.; Albadarin, A.B. Removal of acetaminophen from synthetic wastewater in a fixed-bed column adsorption using low-cost coconut shell waste pretreated with NaOH, HNO₃, ozone, and/or chitosan. *J. Environ. Manag.* **2018**, *226*, 365–376. [[CrossRef](#)]
37. Wu, Q.; Xu, J.; Wu, Z.; Zhu, S.; Gao, Y.; Shi, C. The effect of surface modification on chemical and crystalline structure of the cellulose III nanocrystals. *Carbohydr. Polym.* **2020**, *235*, 115962. [[CrossRef](#)]
38. Milionis, A.; Loth, E.; Bayer, I.S. Recent advances in the mechanical durability of superhydrophobic materials. *Adv. Colloid Interface Sci.* **2016**, *229*, 57–79. [[CrossRef](#)]



© 2020 by the authors. Licensee MDPI, Basel, Switzerland. This article is an open access article distributed under the terms and conditions of the Creative Commons Attribution (CC BY) license (<http://creativecommons.org/licenses/by/4.0/>).